Electronic and structural properties of GaN by the full-potential linear muffin-tin orbitals method: The role of the *d* electrons

Vincenzo Fiorentini,* Michael Methfessel,† and Matthias Scheffler
Fritz-Haber-Institut der Max-Planck-Gesellschaft, Faradayweg 4-6, D-1000 Berlin 33, Germany
(Received 4 September 1992; revised manuscript received 8 February 1993)

The structural and electronic properties of cubic GaN are studied within the local-density approximation by the full-potential linear muffin-tin orbitals method. The Ga 3*d* electrons are treated as band states, and no shape approximation is made to the potential and charge density. The influence of *d* electrons on the band structure, charge density, and bonding properties is analyzed. Due to the energy resonance of Ga 3*d* states with nitrogen 2*s* states, the cation *d* bands are not inert, and features unusual for a III-V compound are found in the lower part of the valence band and in the valence charge density and density of states. To clarify the influence of the *d* states on the cohesive properties, additional full- and frozen-overlapped-core calculations were performed for GaN, cubic ZnS, GaAs, and Si. The results show, in addition to the known importance of core-valence exchange-correlation nonlinearity, that an explicit description of closed-shell interaction has a noticeable effect on the cohesive properties of GaN. Since its band structure and cohesive properties are sensitive to a proper treatment of the cation *d* bands, GaN appears to be somewhat exceptional among the III-V compounds and reminiscent of II-VI materials.

I. INTRODUCTION

Recently, considerable interest has arisen[1] in the wide-gap III-V nitrides as candidates for the realization of devices emitting light in the blue range of the visible spectrum. In particular, successful epitaxial growth of thin films of gallium nitride has recently been demonstrated, resulting in material having the wurtzite or the zinc-blende structure,[2] depending on the substrate.

Although several *ab initio* investigations of this system have appeared recently[3–7] (they are discussed in comparison with our results in a later section), GaN is still relatively poorly known from the theoretical point of view, despite its increasing technological interest. Accurate theoretical predictions are of some relevance in the case of GaN, since characterization and experimental work on this material is still at an early stage when compared to the average development level of III-V technology. The issue of a theoretical description of this system is also of interest in itself, due to the open question about the role of the Ga *d* electrons.

In this work we present calculations of lattice properties and band structure of GaN in the zinc-blende structure (ZB) performed *ab initio* within the local-density approximation (LDA) to the density-functional theory (DFT) exchange-correlation functional[8] using the all-electron full-potential linear muffin-tin orbitals method (FP-LMTO).[9] We analyze the character of band states, density of states, and charge densities, showing the relevance of the Ga *d* shell in determining the properties of the material. Also, we perform full- and frozen-overlapped-core calculations for GaN, ZnS, GaAs, and Si, which enable us to examine the effects of the *d* shell and of other core states on the cohesive properties of the four materials.

In Sec. II we discuss technicalities, in Sec. III some background, in Secs. IV and V the effects of *d* electrons on the band structure and cohesive properties. Section VI compares our results to previous calculations, and Sec. VII displays some relevant aspects of charge densities and wave functions for GaN. Rydberg and bohr atomic units are assumed, unless otherwise specified.

II. TECHNICALITIES

Our calculations were performed within the LDA by the FP-LMTO method[9] using the Vosko-Wilk-Nusair[10] parametrization of the Ceperley-Alder[11] exchange-correlation energy, and the Monkhorst-Pack 10 special-points mesh.[12] The 2*s* and 2*p* states of N and the 3*d*, 4*s*, and 4*p* states of Ga are treated as bands, whereas the remaining core states are self-consistently relaxed in a spherical approximation. As a variational basis for solving the Schrödinger equation, three augmented Hankel functions are used on each occupied atomic site with decay energies −0.7, −1.0, and −2.3 Ry up to angular momentum $l = 2$. This LMTO basis is centered only on the Ga and N spheres (not on the empty spheres; see below), giving 27 functions per atom.

The atomic spheres are nonoverlapping (sphere radii being 97% of half the nearest-neighbor distance) in contrast with the often-used atomic-spheres approximation (ASA) version of the LMTO method.[13] As usual, empty spheres (of the same size as the atomic ones) are inserted in the interstitial regions of the ZB structure to improve the packing fraction.

A full-potential technique needs an accurate evaluation of interstitial three-center integrals and charge density. This is done by an interpolation technique which rep-

resents the product of two Hankel functions as a linear combination of other Hankel functions in the interstitial region. The same technique is used to represent the interstitial exchange-correlation potential and energy density. More details are to be found in Ref. 9. The auxiliary interstitial charge density is expressed as an expansion in Hankel functions with decay energies -1.0 and -3.0 Ry, centered on all spheres, with angular momentum up to $l = 4$.

The results presented below were obtained using a nonrelativistic code. We also performed a scalar-relativistic calculation for GaN with the same method, and the results are found to be essentially unchanged (the lattice constant and fundamental gap are reduced by 0.2% and 1.5%, respectively, and the cohesive energy is practically identical).

III. BACKGROUND

Although GaN is close to being a polytypic material,[1,14] we have not attempted a prediction of the relative stability of ZB and wurtzite structures.[15] The first reason for this is that wurtzite-ZB energy differences are known to be very small both experimentally and computationally in many analogous systems;[16] second, wurtzite is already known to be the stable equilibrium structure of GaN under normal experimental conditions; finally, the existence of an "easy" structural transition induced by the substrate symmetry in epitaxial growth has already been demonstrated experimentally;[1,2] therefore, and also in view of the existence of a synthetic cubic phase of GaN, we consider an analysis of the properties of the cubic phase to be quite relevant at this stage. We note that several theoretical studies have already tackled the problem of phase stability and transformation of GaN,[3–5,7,14] which is not going to be addressed here.

In view of the real-space localization of the valence electrons of N and of the d shell of Ga, the use of an all-electron method, in which electronic states are all treated on equal footing irrespective of their localization properties, appears to be important. In particular, prior to information to the contrary, a proper treatment of the Ga d shell is required. To get an indication of the relevance of these states, one can consider calculations for the free atoms. The approximation of freezing any electronic states in the core, or of eliminating them by a pseudization procedure, can be expected to work only if they are clearly more strongly bound than any of the relevant valence states in the free atom. Further, even if the frozen-core or pseudoatom approximation appears to be reasonable in terms of orbital localization or of depth of eigenvalues, it may break down in a compound crystal due to resonances of the atomic levels of different constituent atoms. An inspection of the free-atom energy levels of Ga and N shows that a special situation occurs in GaN (see Fig. 1). The three uppermost valence bands will originate from the sp states of Ga and the $2p$ electrons of N, the corresponding nonrelativistic full-core free-atom eigenvalues (referred to the ionization limit) being $\epsilon_{4p}^{\mathrm{Ga}} = -2.72$ eV, $\epsilon_{4s}^{\mathrm{Ga}} = -9.12$ eV, $\epsilon_{2p}^{\mathrm{N}} = -7.21$ eV. The lower s valence band should stem from the $2s$ states

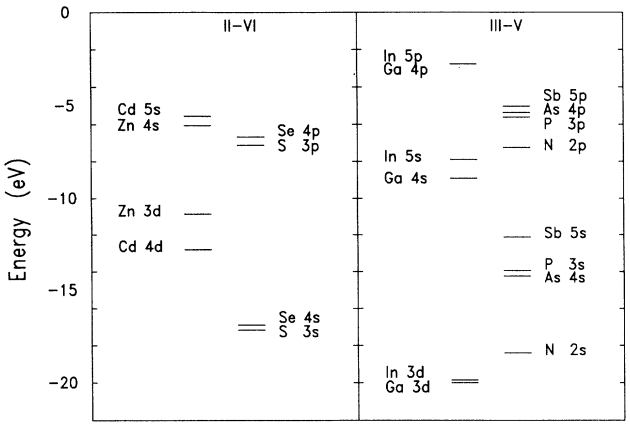

FIG. 1. Nonrelativistic free-atom LDA eigenvalues for some elements involved in the formation of III-V and II-VI compounds.

of N, for which $\epsilon_{2s}^{\mathrm{N}} = -18.37$ eV; interestingly, though, the atomic d states of Ga are found at $\epsilon_{3d}^{\mathrm{Ga}} = -20.0$ eV, in near resonance with the N $2s$ states. From the atomic eigenvalues, one can thus infer that the appearance of d bands must be expected near the lowest, N $2s$-like valence band. Because of the large Ga-Ga distance, we do not expect a direct interaction of Ga $3d$ orbitals, but an indirect one mediated by the resonance with N $2s$ states. This suggests that the proper treatment of the Ga d states as bands is important for understanding the properties of GaN. A recent, comprehensive study of the effects of d states on the properties of II-VI compounds[17] is a useful reference on the problems to be expected in this context.

IV. INFLUENCE OF CATION d STATES ON THE BAND STRUCTURE

To follow up the suggested special role of the cation $3d$ states in GaN, the band structures of three representative compounds are compared in Fig. 2: those of ZnS, GaN, and GaAs. The role of the metal d states is strikingly evident in the GaN band structure (central panel), which turns out to be a borderline case between the typical III-V compound GaAs (bottom) in which practically inert d bands appear well below the s-like bottom valence band, and the typical II-VI compound ZnS (top), in which the d bands lie in the heteropolar gap. In effect, for Zn II-VI compounds such as ZnS, in spite of the relatively limited dispersion, a large hybridization with other states has been shown to be present (e.g., in ZnO,[18] where Zn $3d$ character is as large as 30% to 70% in valence states usually identified as sp states). It is apparent that a proper treatment of the Ga d shell is essential in determining the band structure of GaN. As expected, the d bands are strongly hybridized with the bottom s-like valence band stemming from N $2s$, which results in a large splitting away from the zone center (as sd mixing is symmetry forbidden at Γ). For example, at the L point the bottom valence band (L_1 in Fig. 2) and the lower branch of the upper valence bands (L_1^v in Fig. 2) both belong to

the L_1 representation of the little group of $\mathbf{k}$, C_{3v}; the d bands split into two basically inert L_3^d doublets (one of these originates from the nonbonding Γ_{12}, see figures in Sec. VII), and an L_1 singlet which interacts strongly with the other L_1 bands (see also the discussion in Sec. VII).

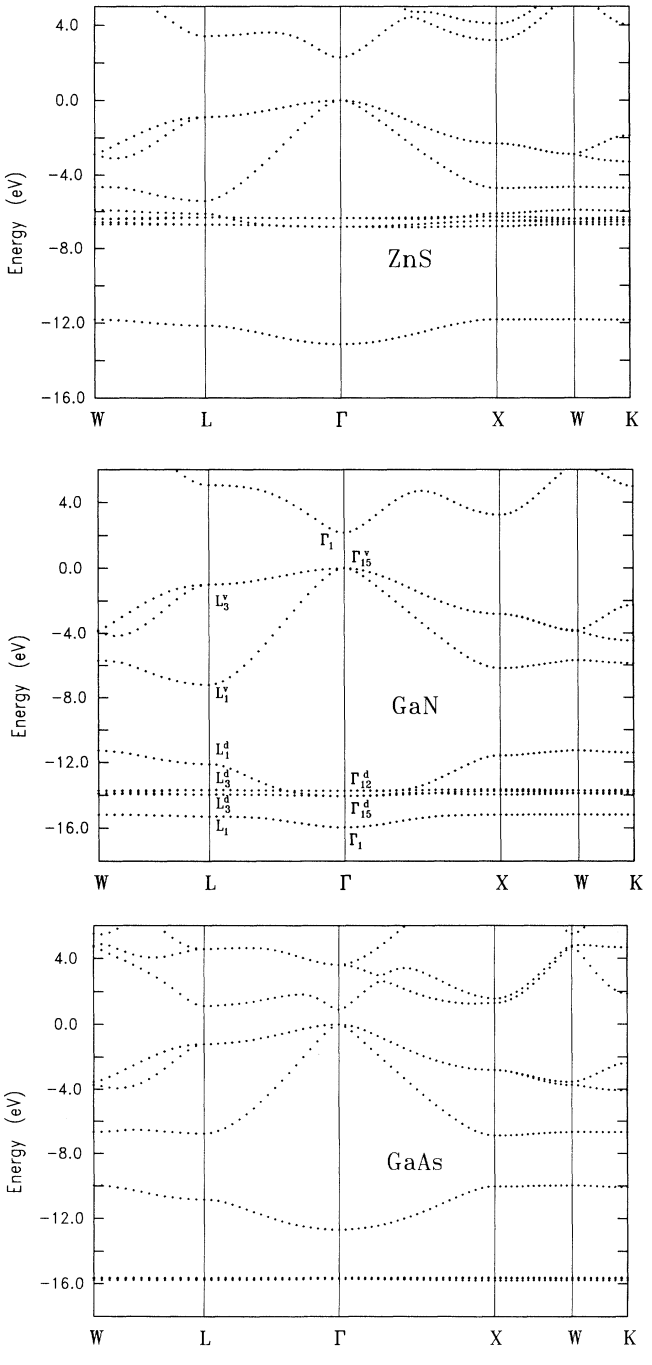

FIG. 2. FP-LMTO band structure of GaN (center), compared to those of ZnS (top) and GaAs (bottom). State labels for the central panel apply straightforwardly to the others. In each panel, the energy zero is the valence-band top. The bands are calculated at the theoretical lattice constants.

To gain some additional insight, it is useful to compare the band structure (Fig. 2) with the atom-projected density of states (DOS) of GaN, for s, p, and d angular momenta, given in Fig. 3. A mesh of 344 special points in the irreducible wedge of the Brillouin zone and a Gaussian broadening of 0.37 eV were used, and the Mullikan decomposition technique[19] was employed (see the Appendix). The s and d bands have contributions from both Ga and N sites, which is a consequence of their hybridization, although most s character still comes from N, whereas most of the d character resides on the Ga site, and is barely sizable on N over the whole valence band (the total charge of d character contributed by the N site is about 0.08 electrons). The N p states dominate the top valence band, but of course *spd* Ga contributions are present as well. The s DOS shows a predominant contribution of N $2s$ to both of the lower bands, and almost none in the upper bands, where some Ga s character is present instead.

Next, in Fig. 4, we show a blow-up of the d bands along the Λ and Δ lines. Along Λ the symmetry is C_{3v}: the Γ_{12} band goes over to a Λ_3 state and remains twofold degenerate, while the Γ_{15} splits into a Λ_3 doublet and a Λ_1 singlet, which interacts with the bottom and top valence bands. Along Δ, the symmetry is C_{4v}, so that Γ_{15} splits into a Δ_5 doublet and a Δ_1 singlet, and Γ_{12} goes into Δ_2 and Δ_1 singlets. The compatibility between the latter and the singlet stemming from Γ_{15} brings about an anticrossing feature with antibonding and nonbonding character being exchanged between the upper and lower levels. The splitting of the hybridized band and the center of mass of the "inert" d bands is 2.03 eV at

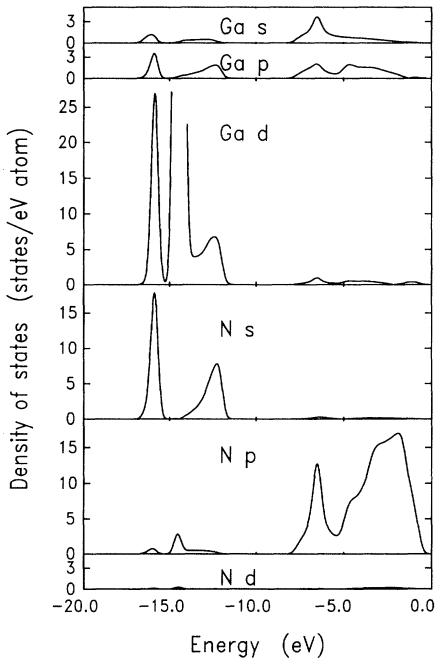

FIG. 3. Mullikan angular momentum decomposition of atom-projected densities of states. From top to bottom: Ga s, p, and d states, and N s, p, and d states.

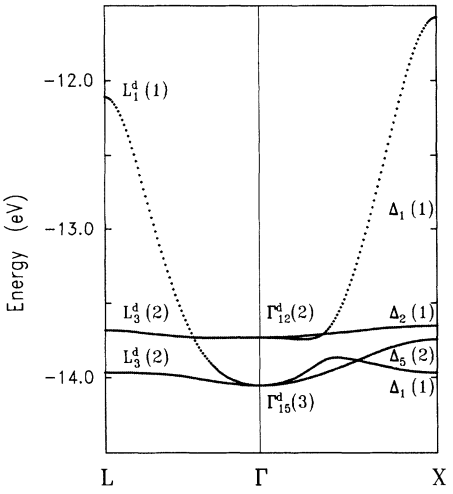

FIG. 4. Detail of the d bands of GaN along L-Γ-X. Degeneracies are indicated in parentheses. Energy scale as in Fig. 2.

X and 1.56 eV at L. It is of some interest to note that these features are an amplification of a pattern present, although less pronounced, in the d bands of ZnS and ZnSe, in accordance with previous all-electron results.[20] Apart from the relative separation of the sd bands, we have observed that as the self-consistency process proceeds, the Ga d levels move up in energy relative to the N s bands, which hardly move at all—that is, the center of mass of the hybridized sd crystal levels is raised in energy with respect to the center of mass of the corresponding atomic levels. This indicates the importance of a self-consistent treatment for the one-electron energies: the global effects of "freezing" the Ga d states (and core levels in general) are discussed in the following section.

The (DFT-LDA) fundamental gap is found to be direct at Γ, $E_g = 2.0$ eV. The experimental value is 3.55 eV in wurtzite GaN, and reported values for cubic GaN range from 3.25 to 3.5 eV.[1,2] An instant estimate of the self-energy correction to the gap[8,21] is provided by a recently proposed simple model,[22] which expresses it as $\Delta \simeq 9/\varepsilon$ eV. Since the high-frequency dielectric constant ε is unknown as yet for the cubic phase, we use the wurtzite phase ε of 5.8, getting a corrected gap of 3.55 eV. The calculated valence-band width is 15.99 eV, which is substantially larger than that of the related compounds GaAs and GaP (13.0 and 13.1 eV, respectively). The main heteropolar gap (s to sp band) is 9.01 eV, while the d-to-sp gap is 5.39 eV (the heteropolar gap in GaAs is 3.44 eV). Apart from d hybridization, these large gaps are to be expected in view of the ionicity of GaN.

V. INFLUENCE OF CATION d STATES ON THE COHESIVE PROPERTIES

The previous section has demonstrated that the Ga d states play an important role in the band structure of GaN, due to strong hybridization with the N $2s$ states near the bottom of the valence band. Still to be ascertained is the importance of these active d bands for the cohesive properties.

Before discussing this point, we report our calculated structural properties of GaN in the ZB structure: $a_0 = 8.44$ bohrs ($\Omega = 150.3$ bohrs^3), $B = 1.98$ Mbar, and $E_{\rm coh} = 10.88$ eV/cell (free-atom spin polarization included). The reported experimental values[1,2] of the lattice constant of zinc-blende GaN average to 8.54 bohrs, resulting in an experiment-theory discrepancy of about 1%, which is usual for LDA calculations on semiconductors. We assume the experimental cohesive energy[5] per formula unit of the wurtzite phase, 9 eV/(Ga-N pair), to be a reasonable estimate of the (as yet unknown) cohesive energy per cell of cubic GaN. The resulting overestimation of the cohesive energy is a known defect of the LDA.[8]

The role of the d electrons is the ensemble of effects which originate from the cation semicore d shell being not inert. In the rest of this section, we endeavor to analyze in which way core states affect the cohesion of several materials, including GaN. The question to be answered is whether a reasonable description of the bonding in GaN can be obtained with an approach which only treats the sp electrons of Ga and N explicitly as band states. In the pseudopotential framework, for example, this is often achieved by simply treating the cation d states as core states and linearizing core-valence exchange and correlation. However, this approach has been shown to fail manifestly for the II-VI compounds, giving lattice constants which are typically 10% to 15% too small.[17,23] In this respect, improved pseudopotential techniques adopt the so-called nonlinear core corrections (NLCC).[24] Hereby the (frozen) free-atom core density is added to the (self-consistent) valence density when the exchange-correlation terms are calculated. This improves things considerably for the II-VI's, since the lattice constant is now only 3% to 4.5% below the experimental value.[23,25] Considering our calculated electronic structure, and especially in view of the work of Min, Chan, and Ho,[4] we postulate that this effect is at least as important for GaN without, however, being in the position of testing this explicitly with our all-electron code.

More generally, the core states can affect the bonding in three distinct ways. *First*, if the core is frozen to its free-atom shape, an (in most cases small) error is made which, according to the variational principle, must increase the total energy, and hence decrease the cohesive energy. This effect disappears when the lattice constant approaches infinity, and it increases monotonically for decreasing lattice constant as long as the core states remain very localized on the typical length scale of the lattice: in the latter regime this effect leads then to an increase of the lattice constant. Thus, core relaxation effectively provides a (weak) interatomic attraction. *Second*, if the core overlaps appreciably with the on-site valence states, the effect of the exchange-correlation nonlinearity sets in, resulting in an interatomic repulsion. *Third*, if the core states are large enough to overlap to some extent (or to interact with neighboring-site filled valence states, as is the case for the Ga d and N s in GaN), the closed-shell repulsion becomes noticeable. This is a consequence

of the increase in the kinetic energy when the cores on neighboring sites are made orthogonal. If this contribution is neglected, the lattice constant comes out too small and the cohesive energy too large. The magnitude of the core-core repulsion effect is governed not only by the overlap of the core wave functions, but also by the amount of resonance between the on-site core eigenvalues for the neighboring sites. This means that the core states can only "see" each other if they are in the same energy range. For a system with neighboring atoms of different types, it is therefore conceivable that there is a reduced closed-shell repulsion if core eigenstates do not resonate. Conversely, for the case of GaN we expect a stronger such repulsion since, as we have seen, there is a rather sharp resonance between the Ga $3d$ and N $2s$ states.

To distinguish between the various core contributions to the bonding, we have done additional calculations using the following technique. In each iteration, the core density is obtained by overlapping the frozen free-atom cores, and the sum of the free-atom core kinetic energies is taken into the total energy. The overlapped cores can extend into the interstitial region and into neighboring atomic spheres. In cases where the core states are localized enough not to overlap, this "frozen–overlapped-core" approximation (FOCA) is identical to the usual frozen-core approximation. For GaN, however, the Ga core is so large compared to the interatomic distance (all Ga core states up to and including the $3d$, are treated as frozen) that a straight frozen-core calculation runs into problems. Of the three core contributions discussed above, the FOCA procedure includes only the nonlinear exchange-correlation contribution; it does not include the core relaxation and closed-shell repulsion effects. It should therefore be closely similar to the pseudopotential-plus-NLCC approach, and should shed light on the applicability of the latter to GaN and related systems.

Table I shows the cohesive properties of GaN, ZnS, GaAs, and Si calculated by the all-electron FP-LMTO method, both with the full treatment and using the FOCA, and compares them to NLCC-pseudopotential (NLCC-PP) results where these are available (the values for GaN are taken from Ref. 4, which we discuss in more detail in the next section). For Si, the core is very small so that the only neglected term in the FOCA is the core relaxation. In agreement with the discussion above, this leads to a slightly larger lattice constant and a smaller cohesive energy. A similar behavior is seen for GaAs, for which the Ga d states are energetically well below the As s states and, in addition, the lattice constant is rather large. The decoupling of the d states is not complete, though, and the relatively small effects of core relaxation and closed-shell repulsion are in competition.

For ZnS as well as GaN, on the other hand, the relevant effect neglected in the FOCA is the closed-shell repulsion with the associated underestimate of the lattice constant and overestimate of the cohesive energy. However, in ZnS the repulsion is between the Zn d and S p states. Although acceptable values are obtained, the lattice constant is still too small by some percent. This is in fact similar to the deviations found when the pseudopotential technique with NLCC is applied, as can be seen from Table I. We note though that the NLCC-PP errors tend to be somewhat larger. This may be attributed in part to the additional approximations needed in the implementation of the NLCC (e.g., the approximation of the core charge inside some inner core radius).

TABLE I. Calculated structural properties for GaN, ZnS, GaAs, and Si in the zinc-blende (diamond) structure. The lattice constant a_0 is in atomic units, B is the bulk modulus in Mbar, and $\delta E_{\rm coh} = E_{\rm coh}^{\rm frozen} - E_{\rm coh}^{\rm full}$ is the difference of cohesive energies (eV/cell) in the frozen-core and full all-electron calculations, respectively. Numbers in parentheses indicate deviations from experimental data.

		All-electron[a]	FOCA[b]	NLCC-PP[c]	Expt.[d]
Si	a_0	10.22 (−0.4)	10.24 (−0.2)		10.26
	B	0.96	0.96		0.99
	$\delta E_{\rm coh}$		−0.41		
GaAs	a_0	10.62 (−0.6)	10.71 (+0.2)	10.50 (−1.7)	10.68
	B	0.75	0.65	0.77	0.77
	$\delta E_{\rm coh}$		0.08		
GaN	a_0	8.44 (−1.2)	8.30 (−2.8)	8.12 (−4.7)	8.54
	B	1.98	2.00	2.40	
	$\delta E_{\rm coh}$		0.33		
ZnS	a_0	10.13 (−0.8)	9.92 (−2.9)	9.80 (−4.0)	10.21
	B	0.75	0.83	1.06	0.77
	$\delta E_{\rm coh}$		0.34		

[a]This work, full FP-LMTO.
[b]This work, frozen overlapped-core FP-LMTO.
[c]Pseudopotentials with nonlinear core corrections (Ref. 4 for GaN, Ref. 23 for ZnS, Ref. 26 for GaAs).
[d]Data from *Numerical Data and Functional Relationships in Science and Technology*, edited by K.-H. Hellwege and O. Madelung, Landolt-Börnstein, New Series, Group III, Vols. 17a and 22a (Springer, New York, 1982), and references therein. For cubic GaN an average of the reported experimental data (Refs. 1 and 2) is used.

We briefly consider the influence of Ga d-shell freezing on the band structure of GaN, in particular on the direct gap, which is 2.00 eV in the full calculation. Although the absence of repulsion between d and top valence p states at zone center causes an increase of the gap (see the detailed discussions in Ref. 17 for II-VI's and 20 for GaAs), a quantitative estimate of gap differences is difficult, due to volume dependences; the high bulk modulus and deformation potentials of the relevant states cause effects similar to those observed for other semiconductors.[27] In our frozen-core calculation we find a gap of 2.66 eV at the frozen-core theoretical lattice constant (8.30 bohrs). When calculated at the theoretical lattice constant of the full calculation (8.44 bohrs), the frozen-core gap is 2.20 eV, 10% larger than the full gap at the same volume. We report in passing our estimate for the deformation potential of the lowest conduction state, 5 meV/kbar, in good agreement with the experimental value of 4.7 meV/kbar.[3]

As a summary of this section, the core states can influence the bonding properties in three ways, namely through core relaxation, nonlinear core-valence exchange-correlation effects, and closed-shell repulsion. To obtain a reasonable description of bonding in II-VI and III-V

semiconductors with d states in the valence range, it is presumably imperative to include nonlinear core corrections in a pseudopotential treatment. The core relaxation has a minor influence and can normally be neglected (apart from cases where accurate cohesive energies are needed). The closed-shell repulsion is rather significant in those cases for which the cation d states are in the same energy range as the anion valence states. As regards the importance of closed-shell repulsion, GaN turns out to be very similar to the II-VI compounds. For all of these materials, a full treatment of the d electrons as band states is needed in order to reduce the remaining $\simeq 4\%$ underestimate of the lattice constant to the LDA-standard $\simeq 1\%$.

VI. COMPARISON WITH PREVIOUS RESULTS

We are now in a position to compare our findings with those of previous investigations of GaN. In the following our calculation is compared with results obtained by others for the zinc-blende structure only. As the only existing all-electron study[3] does not deal directly with zinc blende, we only consider some pseudopotential calculations which have been recently carried out. It is worth reiterating that a comparison of our results with those investigations is not straightforward, due to the problems encountered by pseudopotential methods in treating localized nodeless wave functions such as those of the N $2p$ and Ga $3d$ states, and to the technical differences of the methods.

In the mixed-basis calculation of Ref. 4 a pseudopotential including nonlinear core corrections[24] (NLCC) for the frozen $3d$ shell was used for Ga, and the Bachelet-Hamann-Schlüter (BHS) potential[28] was employed for nitrogen. The adoption of NLCC was found to be necessary, and to improve substantially the transferability of the Ga potential.

A cell volume of 134 bohr^3 (lattice constant $a_0 = 8.12$ bohrs, -3.7% with respect to our result), a bulk modulus of 2.4 Mbar, and a direct gap of 2.8 eV were reported. Since the localized part of the mixed basis can describe reasonably well the nitrogen valence states despite the low plane-wave cutoff of 14 Ry, this severe underestimate of the cell volume could well be due to the approximate treatment of the d shell of Ga. This is consistent with past experience[17] with II-VI's and with our frozen-overlapped core results (previous section). We mention that the reported cohesive energy is only 8.2 eV/cell; as has been argued in Ref. 17, among the effects of partially active d shells there is an increase in lattice constant *and* a reduction of the cohesive energy (see below), so we would expect the pseudopotential cohesive energy to be larger than ours. The much larger gap is partially due to deformation potential effects (the volume being quite small). A further comparison is possible with our calculated frequency of the TO frozen phonon at the zone center, which is $\Omega_{\mathrm{TO}}^{\mathrm{ZB}} = 600$ cm^{-1}. The experimental frequency is not known in cubic GaN, but the analogous mode in the wurtzite structure has $\Omega_{\mathrm{TO}}^{\mathrm{W}} = 533$ cm^{-1}. Although the discrepancy is relatively large ($\simeq 10\%$), part of the problem may lie in wurtzite-ZB differences. As an example, the TO phonon frequency in cubic SiC is known experimentally to be about 10% higher than in hexagonal SiC,[14,31] so this may account for most of the present deviation. On the other hand, the NLCC-pseudopotential result for the *wurtzite* TO frequency ($\Omega_{\mathrm{TO}}^{\mathrm{W}} = 644$ cm^{-1}) obtained in Ref. 4 suffers from a considerably worse discrepancy.

Recently, Palummo *et al.*[5] have studied GaN with plane waves and pseudopotentials, treating the Ga d shell as core states, and linearizing the core-valence exchange-correlation functional (no NLCC). Their results for zinc-blende GaN (requiring a cutoff of 120 Ry) are somewhat puzzling. Using the nitrogen pseudopotential by Gonze, Stumpf, and Scheffler[29] (GSS), they obtain $a_0 = 8.41$ bohrs (-0.5% from our result), $B = 1.69$ Mbar, and $E_{\mathrm{coh}} = 10.25$ eV (-5.7% from ours), whereas they find $a_0 = 8.15$ (-3.4% from our result) and $B = 2.4$ Mbar when using the nitrogen BHS potential, in close agreement with Ref. 4 (the s and p channel of the GSS potential and the s, p, and d channels of the BHS potentials were used, respectively, the last channel listed being included in the local potential). As the authors point out, this important test signals high sensitivity of the results to the specific potential used for nitrogen, possibly due to the high ionicity of the system. This is clearly a potential source of major difficulties, whose effects should be addressed by any similar calculation.

The fundamental gap reported is 2.70 eV, about 0.7 eV larger than ours.[30] This discrepancy could also be attributed to the neglect of the Ga d shell (see the previous section).

The work just cited has indicated that convergence of norm-conserving pseudopotential calculations, especially using standard BHS potentials, requires a very high cutoff. Van Camp, Van Doren, and Devreese[6] used a poorly converged basis ($E_{\mathrm{cut}} = 34$ Ry), which as noted in Ref. 5 makes their results somewhat unreliable. Muñoz and Kunc[7] have used BHS pseudopotentials with a higher cutoff (70 Ry), which, however, is still only 60–70 % of that used by Palummo *et al.*;[5] despite this, and at variance with Ref. 5, they obtain good equilibrium properties for the ZB structure, and a pressure-volume phase diagram in reasonable agreement with that obtained by Gorczyca and Christensen[3] by the all-electron LMTO-ASA method.

In summary, the actual performance of pseudopotential methods as applied to GaN is still rather unclear. Our conclusions from the previous section seem to be essentially valid, namely, that pseudopotential calculations performed without some use of the NLCC can hardly be considered reliable, and that sizable additional improvements appear if the d states are treated self-consistently as band states. The situation is therefore similar to that of II-VI materials, as shown above and in earlier work.[17,23,25] Since the treatment of localized N *and* Ga states in a pseudopotential approach is rather tricky, the satisfactory results obtained for GaN with standard, uncorrected pseudopotential procedures are not easily understandable.

VII. WAVE FUNCTIONS AND DENSITIES

The similarity of GaN and the prototypical II-VI ZnS has been observed in the band structure and cohesive properties. Such effects are due to the cation d shell being not inert in these systems. To render this visually, we present a selection of partial charge densities for GaN. This is similar in spirit to the work of Wei and Zunger,[17] who have investigated in some detail the effect of cation d states on (among others) the charge densities of selected states and on the total densities in several II-VI compounds. Charge densities at specific $\mathbf{k}$ points [the modulus squared of the wave function $\psi_i(\mathbf{k},\mathbf{r})$ at $\mathbf{k}$] as well as $\mathbf{k}$-integrated band contributions to the density will also be considered. All charge densities are plotted in a (110) plane. For convenience, superscripts d and v are used to label states originating from d bands and uppermost valence bands, respectively, whereas states with no superscripts are from the bottom valence band. Density plots have the lowest contour and contour spacing of 0.5 and 1 electron/cell, respectively. Wave functions have been symmetrized. The reader should refer to Fig. 2 for a guide to the relevant band state labels, and to Fig. 3 (DOS) for the hybridization of different angular-momentum characters.

In the zinc-blende structure, the mixing of p and d states is permitted[17] even at the Γ point, which has T_d as a group of $\mathbf{k}$ (contrary to the situation in the diamond structure, where it has the full O_h symmetry). The upper valence bands at Γ will no longer have the character of a bonding combination of p orbitals, antibonding d character being admixed into them; conversely, the d bands will contain p components. The mixing of s and d states is not allowed at Γ, but at a general $\mathbf{k}$ point of lower symmetry, states with all symmetries of the rotation group will in general be allowed to interact. Therefore, charge density and density of states (which are obtained by averaging over the Brillouin zone), and the full band structure will be only partially reminiscent of the specific symmetry of the original atomic states. This is the case, e.g., for the Γ_{15}^d triplet of d origin which is only p-admixed at the zone center, but gives rise to a strongly s- and p-admixed singlet away from the zone center, and for the Γ_1 s-like singlet, which is similarly admixed with pd character away from Γ. Already at the zone center, the ordering of the d-like Γ_{15} triplet and Γ_{12} doublet (which remains practically inert throughout the zone, resulting

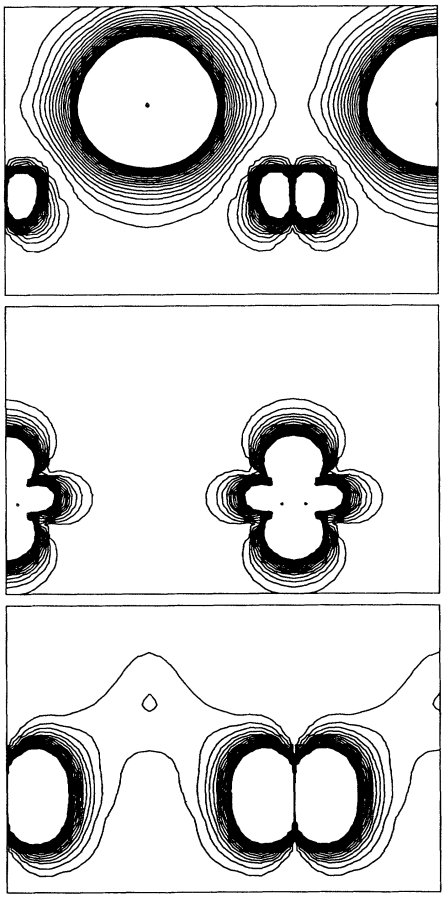

FIG. 5. Squared wave functions of the states Γ_{15}^v (top), Γ_{12}^d (center), Γ_{15}^d (bottom) at the zone center in GaN (see text).

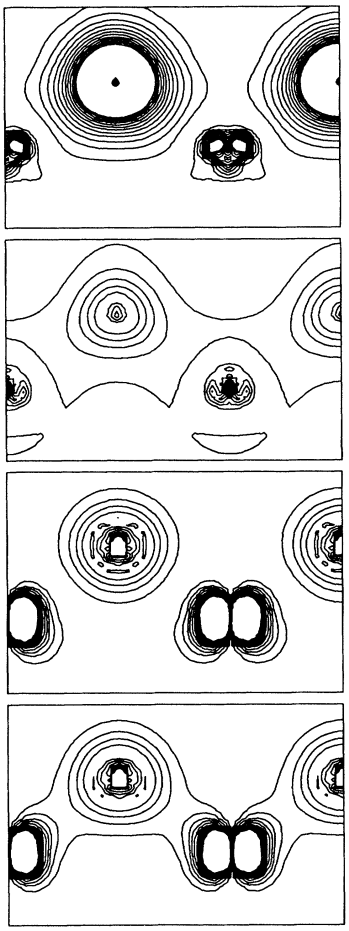

FIG. 6. Symmetrized squared wave functions of the states L_3^v, L_1^v, L_1^d, and L_1 (top to bottom) at the L point in GaN.

in a nonbonding state) is reversed with respect to what is expected[32] for a tetrahedral environment, due to *pd* repulsion with the top valence band. Qualitative schemes of the *pd* interaction are given in Ref. 17.

In Fig. 5 we plot the squared wave functions at the zone center for the states $\Gamma_{15}^d, \Gamma_{12}^d$, and Γ_{15}^v in GaN. The former two states originate from the tetrahedral splitting of atomic d states (the fivefold degenerate d multiplet is split in a Γ_{15} triplet and a Γ_{12} doublet), the latter is the bonding p-like valence state. The Γ_{12} state remains very similar to a $d_{z^2-r^2}$-like atomic orbital and forms a nonbonding, inert state. In the other states, the prevailingly ionic character of the bonding is visible; the admixture of Ga d_{xz}-like and N p character results in a weak bonding contribution to Γ_{15}^d and an antibonding one to Γ_{15}^v.

While at zone center only *pd* mixing is allowed, this restriction does not apply to lower-symmetry points. We consider as representative the squared wave functions at the L point. There, the bottom valence band is of L_1 symmetry; the Γ_{15}^d triplet splits further into an L_3^d doublet, analogous to the (Γ_{12})-L_3^d, and an L_1^d singlet. Figure 6 shows the symmetrized squared wave function at L (the average over the eight equivalent L points in the Brillouin zone), for the states L_1, L_1^d, L_1^v, L_3^v (top to bottom). We notice that the bottom, formerly s-like, valence state L_1 has a bonding d admixing, and L_1^d and L_3^v have it antibonding instead.

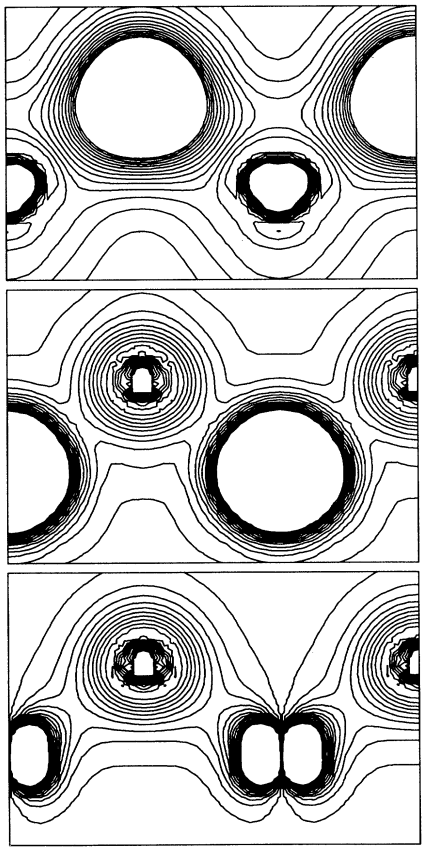

FIG. 7. Partial k-integrated charge densities in GaN for the top valence bands (top), d bands (center), and bottom valence band (bottom).

Next, in Fig. 7 we plot the **k**-integrated partial charge densities $n_i(\mathbf{r})$ for the bottom, d, and top valence bands. The first two are *sd*-like and have some bonding contribution from the Ga d-like states, the latter is ionic p-like and has an antibonding d_{xz}-like admixing, which is visible as a depletion along the bond direction. As expected the Brillouin zone summation has brought about a mixing of all angular momenta (in particular *sd* in the two lower bands). The top valence states are clearly dominated by ionic charge transfer.

Finally, we compare GaN to ZnS and GaAs in Fig. 8. Shown for the three materials (top to bottom: ZnS, GaN, GaAs) are the states Γ_{15}^v (right) and the **k**-integrated densities of the bottom valence-band (center) and of the top valence-band complex (left). The similarity of GaN and ZnS is remarkable. The effect of d admixing is more visible in the ZnS top valence charge, as the d bands are close to and significantly hybridized with the top valence bands.[18] The bonding contribution of the d electrons to the ionic bottom valence charge is instead stronger in GaN, as here the hybridization of s and d bands is larger. The top valence-band, zone-center state Γ_{15}^v (right) shows a conspicuous antibonding contribution of the d electrons, of a similar kind in ZnS and GaN. Even in GaAs, though, a slight d admixing is visible in this state (analogous to that observed recently[33] in InP, InAs, and InSb) and its bottom valence charge also shows some d component. We should mention that ionicity is only partially responsible for the differences between GaAs and GaN, or the similarities of ZnS and GaN, as the ionicity of GaN is 0.43 as compared to 0.33 of GaAs and 0.70 of ZnS.[3] It is interesting to compare directly the partial-density features with the results of Ref. 17 for II-VI compounds.

We conclude that in contrast to most other III-V compounds (represented here by GaAs), GaN does exhibit features of the charge densities and band structure which resemble those observed[17] for II-VI's (represented here by ZnS). This is again due to the Ga d shell resonating with the N s levels, leading to similar effects as the Zn d – anion p interaction.

VIII. SUMMARY

We have calculated the properties of β-GaN using the *ab initio* LDA all-electron full-potential LMTO method. The explicit consideration of the d electrons of Ga has been shown to be of some importance in precisely determining the properties of the material. Due the resonance of N s and Ga d states, the band structure, DOS, and charge density of GaN are quite peculiar for a III-V compound, as significant $3d$ character is present in the valence bands. Several features of GaN of the band structure, charge density, and density of states do actually resemble those of II-VI materials.

A frozen overlapped-core procedure was used to identify the way in which the core and d states influence the cohesive properties of GaN as compared to some other relevant materials. We deduce that, although exchange-

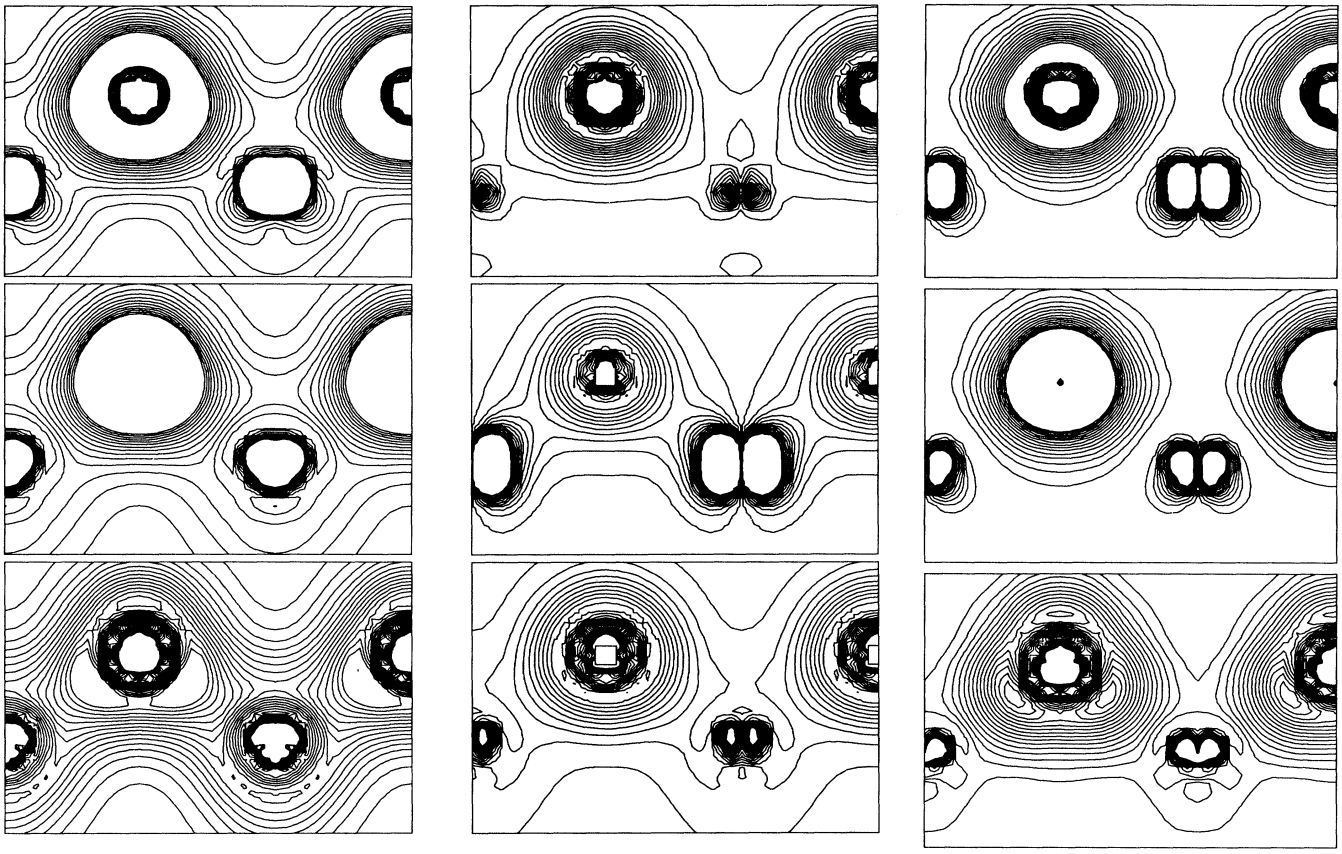

FIG. 8. Comparison of ZnS (top row), GaN (center), and GaAs (bottom). Right column: state Γ_{15}^{v}; central column: bottom valence-band partial density; left column: top valence-band partial density.

correlation nonlinearity is the most important effect in GaN and ZnS, the closed-shell repulsion also plays a significant role; neglect of this effect leads to an additional reduction of the lattice constant by approximately 2% relative to experiment. This sets an upper limit on the accuracy which can be expected of methods which do not treat the d states explicitly. Pseudopotentials including nonlinear core corrections go a long way in the right direction, but generally may not be sufficient for a description of GaN, as well as of ZnS and similar systems, at the standard LDA level of accuracy for semiconductors.

Note added in proof. It has been brought to our attention that the need for a self-consistent treatment of d states in this compound was independently pointed out by W. L. Lambrecht and B. Segall, in *Diamond, Boron Nitride, Silicon Carbide, and Related Wide Bandgap Semiconductors*, edited by J. T. Glass, R. F. Messier, and N. Fujimori, MRS Symposia Proceedings No. 242 (Materials Research Society, Pittsburgh, 1992), p. 367.

APPENDIX: MULLIKEN DECOMPOSITION

Mixing of all angular momenta takes place in the crystal environment due to symmetry lowering, but the content of a specific angular momentum character of a crystal state can still be analyzed. A technique which allows monitoring the site and angular-momentum dependence of the charge distribution is the Mulliken decomposition[19] of the total density of states. The total DOS can be decomposed into site and angular momentum contributions, and if desired, into bonding and antibonding overlaps. Such a population analysis is particularly appropriate for a localized basis such as that used here, and it is expected to be particularly accurate when a linearized partial-wave basis, specifically LMTO's, is used.

The LMTO basis set naturally gives a decomposition of the calculated wave functions as a sum over sites and angular momenta as $\psi(\mathbf{r},\mathbf{k}) = \sum_{\nu L} \psi_{\nu L}(\mathbf{r},\mathbf{k})$, where ν is a site index and L a composite angular momentum index. We then take the decomposition of the norm, giving weights to add into the partial densities of states, as

$$1 = \langle\psi(\mathbf{k})|\psi(\mathbf{k})\rangle = \sum_{\nu L} \mathrm{Re}\left[\langle\psi(\mathbf{k})|\psi_{\nu L}(\mathbf{k})\rangle\right]. \qquad \text{(A1)}$$

The advantage of this approach over the common technique of projecting onto angular momenta inside atomic spheres is twofold: first, the decomposition is only weakly dependent on sphere radii, and second, no DOS contribution is associated with the empty spheres or the interstitial region.

* Permanent address: Dipartimento di Scienze Fisiche, Università di Cagliari, via Ospedale 72, I-09100 Cagliari, Italy.
† Present address: Institut für Halbleiterphysik, Walter-Korsing-Strasse 2, O-1200 Frankfurt/Oder, Germany.

[1] R. F. Davis, Proc. IEEE **79**, 702 (1991).
[2] M. J. Paisley, Z. Sitar, J. B. Posthill, and R. F. Davis, J. Vac. Sci. Technol. A **7**, 701 (1989); R. C. Powell *et al.*, in *Diamond, Boron Nitride, Silicon Carbide and Related Wide Bandgap Semiconductors*, edited by J. T. Glass, R. F. Messier, and N. Fujimori, MRS Symposia Proceedings No. 162 (Material Research Society, Pittsburgh, PA, 1990), p. 525; M. Mizuta, S. Fujieda, Y. Matsumoto, and T. Kavamura, Jpn. J. Appl. Phys. **25**, L945 (1986); G. Martin, S. Strite, J. Thornton, and H. Morkoc, Appl. Phys. Lett. **58**, 2375 (1991).
[3] P. Perlin, I. Gorczyca, N. E. Christensen, I. Grzegory, H. Teisseyre, and T. Suski, Phys. Rev. B **45**, 13 307 (1992); I. Gorczyca and N. E. Christensen, Solid State Commun. **80**, 335 (1991).
[4] B. J. Min, C. T. Chan, and K. M. Ho, Phys. Rev. B **45**, 1159 (1992).
[5] M. Palummo, C. M. Bertoni, L. Reining, and F. Finocchi, Physica B (to be published).
[6] P. E. Van Camp, V. E. Van Doren, and J. T. Devreese, Solid State Commun. **81**, 23 (1992).
[7] A. Muñoz and K. Kunc, Phys. Rev. B **44**, 10 372 (1991).
[8] R. Dreizler and E. K. U. Gross, *Density Functional Theory* (Springer, Berlin, 1990).
[9] M. Methfessel, Phys. Rev. B **38**, 1537 (1988); M. Methfessel, C. O. Rodriguez, and O. K. Andersen, *ibid.* **40**, 2009 (1989). See also M. Methfessel and M. Scheffler, Physica B **172**, 175 (1991), for an application to semiconductor interfaces.
[10] S. H. Vosko, L. Wilk, and M. Nusair, Can. J. Phys. **58**, 1200 (1980).
[11] D. M. Ceperley and B. J. Alder, Phys. Rev. Lett. **45**, 566 (1980).
[12] H. J. Monkhorst and J. D. Pack, Phys. Rev. B **13**, 5188 (1976).
[13] O. K. Andersen, O. Jepsen, and D. Glötzel, in *Highlights of Condensed Matter Theory*, edited by F. Bassani, F. Fumi, and M. P. Tosi (North-Holland, Amsterdam, 1985).
[14] C.Y. Yeh, Z. W. Lu, S. Froyen, and Alex Zunger, Phys. Rev. B **45**, 12 130 (1992), and references therein.
[15] The feasibility of FP-LMTO calculations in strained and complicated geometries for semiconductors has been previously demonstrated (Ref. 9).
[16] Typical calculated total energy differences between wurtzite and zinc blende are fractions of mRy per atom, and are quite sensitive to technicalities as **k**-point summation [for example, a too coarse **k**-point mesh tends to spuriously stabilize (Ref. 14) the zinc-blende structure].
[17] S.-H. Wei and A. Zunger, Phys. Rev. B **37**, 8958 (1988).
[18] A. Catellani, A. Baldereschi, and M. Posternak (unpublished).
[19] R. S. Mulliken, J. Chem. Phys. **23**, 1833 (1955); T. Hughbanks and R. Hoffmann, J. Am. Chem. Soc. **105**, 3528 (1983).
[20] The features of the bands of ZnS and GaAs are in quite good agreement with previous calculations [see, e.g., the LMTO calculation by G. B. Bachelet and N. E. Christensen, Phys. Rev. B **31**, 879 (1985), for GaAs, and the FLAPW results of A. Continenza, S. Massidda, and A. J. Freeman, *ibid.* **38**, 12 996 (1988), for ZnSe]. LAPW and pseudopotential calculations (the latter including the *d* electrons in the valence) have been performed for ZnS by J. L. Martins, N. J. Troullier, and S.-H. Wei, Phys. Rev. B **43**, 2213 (1991).
[21] See, e.g., R. W. Godby, L. J. Sham, and M. Schlüter, Phys. Rev. B **37**, 10 159 (1988).
[22] V. Fiorentini and A. Baldereschi, J. Phys. Condens. Matter **4**, 5967 (1992).
[23] G. E. Engel and R. J. Needs, Phys. Rev. B **41**, 7876 (1990).
[24] S. Froyen, S. G. Louie, and M. L. Cohen, Phys. Rev. B **26**, 1738 (1982).
[25] A. Kley, J. Neugebauer, and M. Scheffler (unpublished).
[26] M. Peressi (unpublished). The NLCC pseudopotentials were generated by A. Dal Corso and P. Giannozzi.
[27] V. Fiorentini, Phys. Rev. B **46**, 2086 (1992); Solid State Commun. **83**, 871 (1992).
[28] G. B. Bachelet, D. Hamann, and M. Schlüter, Phys. Rev. B **26**, 4199 (1982).
[29] X. Gonze, R. Stumpf, and M. Scheffler, Phys. Rev. B **44**, 8503 (1991).
[30] Of course an accurate estimate of the LDA gap is essential to the calculation of quasiparticle energies.
[31] L. Patrick, D. R. Hamilton, and W. J. Choycke, Phys. Rev. **143**, 526 (1966).
[32] B. Figgis, *Introduction to Ligand Fields Theory* (Interscience, New York, 1966).
[33] S. Massidda, A. Continenza, A. J. Freeman, T. M. De Pascale, F. Meloni, and M. Serra, Phys. Rev. B **41**, 12 079 (1990).